APPENDIX E

Multiplicities of Secondaries in Interactions of 1.8 GeV/Nucleon ^{56}Fe Nuclei with Photoemulsion and the Cascade Evaporation Model

by

V.E. Dudkin, E.E. Kovalev, N.A. Nefedov
V.A. Antonchik, S.D. Bogdanov, V.I. Ostroumov
H.J. Crawford and E.V. Benton

MULTIPLICITIES OF SECONDARIES IN INTERACTIONS OF 1.8 GeV/NUCLEON ^{56}Fe NUCLEI WITH PHOTOEMULSION AND THE CASCADE EVAPORATION MODEL

V.E. DUDKIN, E.E. KOVALEV and N.A. NEFEDOV

Institute of Biomedical Problems of the Ministry of Public Health of the USSR, Moscow, USSR

V.A. ANTONCHIK, S.D. BOGDANOV and V.I. OSTROUMOV

Leningrad Polytechnical Institute, Leningrad, USSR

H.J. CRAWFORD

University of California Space Sciences Laboratory, Berkeley, CA 94720, USA

E.V. BENTON

Physics Department, University of San Francisco, San Francisco, CA 94117, USA

Abstract: A nuclear photographic emulsion method was used to study the charge-state, ionization, and angular characteristics of secondaries produced in inelastic interactions of ^{56}Fe nuclei at 1.8 GeV/nucleon with H, CNO, and AgBr nuclei. The data obtained are compared with the results of calculations made in terms of the Dubna version of the cascade evaporation model (DCM). The DCM has been shown to satisfactorily describe most of the interaction characteristics for two nuclei in the studied reactions. At the same time, quantitative differences are observed in some cases.

1. Introduction

Nuclear collisions at high energies keep arousing considerable interest because of the search for feasible manifestations of unusual properties of nuclear matter under conditions of high pressure and high temperatures. The great number of proposed theoretical approaches to describing the inelastic interaction of two nuclei [1]) make it obviously necessary to carry out a detailed quantitative comparison of experimental data on nucleus-nucleus interactions with the predictions of various models.

The present work compares the experimental data on the charge-state, ionization, and angular characteristics of the secondaries produced in the collisions of ^{56}Fe nuclei with hydrogen, light (CNO) and heavy (AgBr) components of photographic

emulsion with the calculation results obtained in terms of the Dubna version of the cascade model (DCM).

2. Experiment and model

The experimental data has been obtained by studying a NIKFI BR-2 emulsion chamber irradiated by 1.9 GeV/nucleon Fe ions at the Lawrence Berkeley Laboratory BEVALAC. Interactions were sought by double (fast and slow) scanning of tracks. At a 112.77 m length, 1478 events were recorded from which a 7.63 ± 0.21 cm mean free path was inferred. The range-energy dependence was used [2]) to find the mean energy of the collision-initiating nuclei which proved to be 1.8 GeV/nucleon.

The energy and specie of the secondaries were inferred from the measured track lengths and from ionization loss. The ionization parameters (I) were taken to be the grain density per unit track length at $I < 9I_0$ (where I_0 is the minimum ionization of a singly-charged particle) and the number of ocular scale intervals closed by grain conglomerates on unit track length (at $I > 4I_0$) [3]). The charged particles which stopped in emulsion were identified using the relation between the specific ionization loss and the residual range. The ionization loss variation on a visible range length was determined for the particles ejected from the chamber.

The charges of the fragments of projectile nuclei were found by three methods, namely, by measuring the grain density, the lacunarity and the δ-electron number density. In this way, the energy of the initiating nucleus and the ejection angles and charges of all secondaries were found for each of the processed interactions.

In accordance with the emulsion terminology, all secondaries in stars were classified into black (b) particles with energy $E_p \leq 26$ MeV; gray (g) particles with $26 < E_p \leq 400$ MeV; stream (s) particles with $E_p > 400$ MeV; heavily ionizing (h) particles from target break-up; and fragments of projectile nuclei [4]). It should be noted also that the relativistic single-charged particles whose emission angle is below $5°$ ($\theta < 5°$) were treated as singly-charged fragments of a projectile nucleus and were not regarded as s-particles. The total charge of non-interacting fragments of the projectile nucleus $Q = \sum_i n_i Z_i$ was determined in each interaction [n_i is the number of fragments with charge Z_i (at $\theta < 5°$); the summation is with respect to all such fragments in an event]. In accordance with the classification adopted in cosmic-ray physics, the charge spectrum of the fragments was broken into the following groups: group L ($3 \leq Z \leq 5$), group M ($6 \leq Z \leq 9$), group H ($10 \leq Z \leq 19$), and group vH ($20 \leq Z \leq 26$). Also, the singly- and doubly-charged fragments (p and α, respectively) were discriminated.

The measurements were made from 558 inelastic interactions of iron nuclei with emulsion nuclei. Out of these, 314 interactions were selected without any discrimination. Also selected were 244 stars (processed to increase the ensemble of events in the hydrogen and light nuclei of emulsion) consisting of fewer than 11 particle fragments emanating from target nuclei ($n_h \leq 10$). The criteria developed in ref. [5])

were used to classify the events into three groups according to the target-nucleus specie, namely, the ^{56}Fe interactions with hydrogen (H) and with light (CNO) and heavy (AgBr) nuclei in emulsion which included 107, 228 and 162 events, respectively.

The calculations were made in terms of the DCM [6-8] allowing for the meson production processes, for the Lorentz compression, for the Pauli exclusion principle, and for the effect of nucleon matter density variations as a cascade develops. The process of removing the excitation of nuclear residues after completing the fast stage was described in terms of a statistical model [9]. The calculational statistics were obtained by Monte Carlo interactions for the H, C, N, O, Ag and Br targets, which were summed up afterwards with the weights corresponding to the calculated cross sections for inelastic nucleus–nucleus interactions and to the elemental composition of emulsion. In all, 4767 events were simulated.

3. Interaction cross sections

The experimental probabilities for iron nuclei to interact with hydrogen and with light and heavy nuclei in the emulsion were $(16.6 \pm 0.8)\%$, $(35.6 \pm 1.7)\%$ and $(47.8 \pm 2.6)\%$, respectively. The effective cross sections for disintegration of nuclei with similar masses may be approximately assumed to be proportional to their geometric dimensions, thereby making it possible to calculate the interaction cross sections for each of the elements separately if the elemental composition of the emulsion and the measured mean free path of iron nuclei in the emulsion are known (see table 1). Table 1 presents also the effective cross sections calculated in terms of the DCM and by the Bradt–Peters formula [10]:

$$\sigma_{in} = \pi r_0^2 [A_1^{1/3} + A_2^{1/3} - B(A_1^{-1/3} + A_2^{-1/3})]^2, \tag{1}$$

TABLE 1

Comparison of the measured inelastic cross sections (in barns) with those calculated using DCM and formula (1) for 1.8 GeV/nucleon ^{56}Fe incident on photoemulsion nuclei

Target	Experiment	Calculation DCM	Calculation formula (1)
H	0.74 ± 0.07	0.75 ± 0.02	0.77 ± 0.02
C	1.75 ± 0.11	1.82 ± 0.05	1.67 ± 0.04
N	1.80 ± 0.12	1.93 ± 0.07	1.76 ± 0.04
O	1.86 ± 0.13	2.04 ± 0.08	1.83 ± 0.04
Br	3.09 ± 0.26	3.17 ± 0.10	3.26 ± 0.08
Ag	3.30 ± 0.28	3.53 ± 0.14	3.65 ± 0.08
CNO	1.80 ± 0.12	1.93 ± 0.07	1.74 ± 0.04
AgBr	3.24 ± 0.27	3.35 ± 0.11	3.46 ± 0.08

where A_1 and A_2 are masses of projectile nucleus and of target-nucleus, respectively; $r_0 = 1.32$ fm; $B = 0.85$.

It can be seen that the presented experimental and DCM-calculated cross sections are in agreement within statistical errors. The results are also close to the data obtained elsewhere. For example, the cross sections for inelastic interactions of ^{56}Fe nuclei with hydrogen, carbon, and silver at a similar energy presented in ref. [11]) are 0.68 ± 0.04, 1.56 ± 0.05 and 3.34 ± 0.08 b, respectively; in ref. [9]), the cross section for pFe collisions at 2.8 GeV was found to be 0.69 ± 0.03 b.

The results of calculating the cross sections for nucleus-nucleus collisions by the formula (1) which approximates the well-known data on relativistic projectile nuclei of lower masses [12]) proved to agree satisfactorily with the cross sections obtained in the present experiment. This fact makes it possible to extend the application scope of (1) to the projectile masses $A_1 = 56$.

4. Fragmentation of projectile nucleus

Table 2 presents the cross sections for fragmentation of iron nuclei on the various emulsion components. It is seen that the fragmentation cross section depends strongly on the target-nucleus specie. In ref. [13]), where the 2.1 GeV/nucleon ^{12}C and ^{16}O fragmentation was studied, the cross section for production of a projectile-nucleus fragment, σ^f_{PT}, was presented as

$$\sigma^f_{PT} = \gamma_T \gamma^f_P, \tag{2}$$

where γ_T is a target factor (defined by the properties of a given target-nucleus and with the dimension of cross section), and γ^f_P is the factor describing fragmentation of projectile P into fragment f. On the above-mentioned assumptions, the ratio of the fragment yields of identical groups for different target nuclei is defined solely by the ratio $\gamma_{T_1}/\gamma_{T_2}$ (where γ_{T_1} and γ_{T_2} are factors of the first and second targets) and does not depend on the fragment type. Studying the cross sections for production of fragments with $Z = 18$-24 in the interactions of iron nuclei of the same energy with various targets [11]) has yielded the target factors of 1.4 ± 0.1, 1.9 ± 0.09, and

TABLE 2 -

Fragmentation cross sections (barns) for 1.8 GeV/nucleon ^{56}Fe interacting with different types of photoemulsion nuclei

Target	Type of fragment					
	p $(Z = 1)$	α $(Z = 2)$	L $(3 \le Z \le 5)$	M $(6 \le Z \le 9)$	H $(10 \le Z \le 19)$	vH $(20 \le Z \le 26)$
H	2.22 ± 0.14	1.03 ± 0.10	0.10 ± 0.02	0.10 ± 0.02	0.33 ± 0.04	0.34 ± 0.04
CNO	7.02 ± 0.57	3.38 ± 0.31	0.36 ± 0.06	0.38 ± 0.06	0.50 ± 0.08	0.49 ± 0.06
AgBr	10.70 ± 0.72	4.54 ± 0.49	0.62 ± 0.08	0.29 ± 0.09	0.32 ± 0.13	0.91 ± 0.18

2.94 ± 0.14 for the Fe + H, Fe + C, and Fe + Ag collisions, respectively. The γ_H/γ_C and γ_C/γ_{11g} values are then, 0.73 ± 0.06 and 0.65 ± 0.06 and appear to be close to the values 0.84 ± 0.08 and 0.69 ± 0.06 obtained in our experiment for the respective range of fragment charges ($Z = 18-24$).

To allow for the transformation of the charge state of cosmic rays as they traverse matter, it is necessary to know, to within as high an accuracy as possible, the mean production multiplicities of fragments (the fragmentation parameters, P_{ij}) which are defined to be the mean numbers of fragments of type j produced in disintegration of a projectile nucleus of type i. Table 3 presents the fragmentation parameters for the collisions of iron nuclei with emulsion nuclei (em) and with its components. Fig. 1 shows the distribution of the number of secondary fragments in an interaction event for the Fe + em disintegrations.

The inelastic nuclear collisions in an emulsion are usually studied using the criterion of discrimination of "central" interactions which means that any charged fragments of a projectile nucleus must be absent in a star. In our experiment, the events of this type amounted to less than 2%. At the same time, the number of singly-charged fragments in an interaction event may reach 12, while the numbers of doubly-charged fragments and the fragments with charges exceeding three may be 6 and 3, respectively, thereby indicating a very strong feasible excitation of the projectile-nucleus residue after the first interaction stage.

An increase in the target-nucleus mass results in a decreased fraction of disintegrations with multicharge fragments ($Z \geq 3$). The values of $P_{Fe, Z \geq 3}$ are 1.17 ± 0.04, 0.96 ± 0.04, and 0.76 ± 0.04 for the H, CNO, and AgBr targets, respectively. Also, it should be noted that a noticeable number of events with two and more $Z \geq 4$ particles

TABLE 3

Comparison of experimental fragmentation parameters to the results calculated using fireball phenomenology (shown in parentheses) for 1.8 GeV/nucleon ^{56}Fe interacting with different types of photoemulsion nuclei

Type of fragment	Type of interaction			
	Fe + H	Fe + CNO	Fe + AgBr	Fe + em
p	3.00 ± 0.19	3.90 ± 0.18 (2.96)	3.2 ± 0.2 (1.43)	3.4 ± 0.1 (2.35)
α	1.39 ± 0.14	1.88 ± 0.11 (1.02)	1.4 ± 0.2 (0.75)	1.6 ± 0.1 (0.81)
L	0.14 ± 0.03	0.20 ± 0.03 (0.12)	0.19 ± 0.04 (0.14)	0.12 ± 0.05 (0.13)
M	0.13 ± 0.04	0.21 ± 0.03 (0.12)	0.09 ± 0.03 (0.12)	0.10 ± 0.03 (0.10)
H	0.44 ± 0.05	0.28 ± 0.04 (0.46)	0.10 ± 0.04 (0.42)	0.20 ± 0.03 (0.40)
vH	0.46 ± 0.05	0.27 ± 0.03 (0.30)	0.28 ± 0.05 (0.12)	0.29 ± 0.03 (0.23)
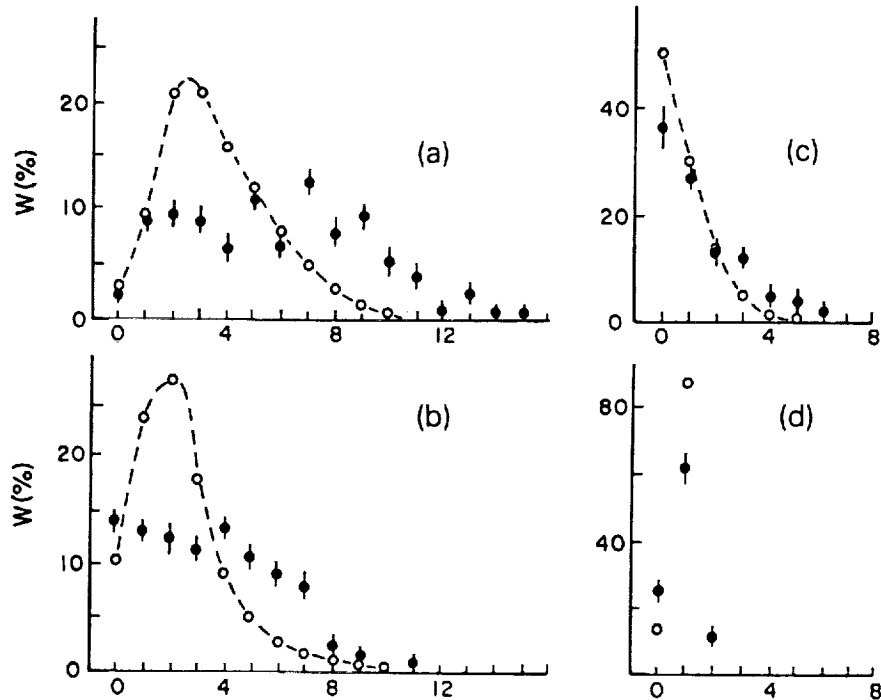
Fig. 1. Relative probabilities for a definite number of the ^{56}Fe fragments with charges $Z \geqslant 1$ (a), $Z = 1$ (b), $Z = 2$ (c) and $Z \geqslant 3$ (d) to occur in collision with emulsion nuclei at a 1.8 GeV/nucleon projectile energy. The full dots are experimental data; the open dots are calculated results of the model [17].

ejected at small angles ($\theta \leqslant 2°$) were observed in the ^{56}Fe + H collisions. The occurrence frequency of such stars was $(12 \pm 3)\%$.

The results obtained for fragmentation of iron nuclei on hydrogen may be explained by examining the data on production of heavy fragments of a target nucleus in the "mirror" p + Fe collision at the same energies of incident proton. According to ref. [14], the probability for the $Z \geqslant 4$ fragments to be ejected at $E_p = 2$ GeV from heavy nuclei of an emulsion is $(4 \pm 1)\%$. The presence of two and more multicharged particles belonging to a projectile nucleus in the Fe + H collisions may, then, be interpreted to be indicative of the process of Fe target-nucleus fragmentation in a "mirror" reaction. In this sense, a multicharged particle of the highest charge may be defined to be a residue nucleus, while the remaining such particles are regarded as fragments.

The validity of the above assumption is corroborated by the fact that the charged-particle multiplicity in the Fe + H events with a single multicharged fragment and with two such fragments was 7.82 ± 0.39 and 11.61 ± 0.76, respectively. The same dependence was also observed in the case of the initiating protons [15]; namely, the multicharged fragment ejection probability increases with the disintegration degree of a target nucleus. The total multiplicity of singly- and doubly-charged particles, which characterizes the Fe nucleus excitation degree, also increases when going over from the disintegrations with a single multicharged particle to the stars with two such particles (from 4.1 ± 0.3 to 5.9 ± 0.7, respectively).

Thus, studying the disintegrations with two and more multicharged particles may yield unique information for examining the nuclear fragmentation process. In this case, hydrogen is expedient to use as targets because the occurrence probability of stars with two large fragments in the Fe + H collisions is three times as high as in the Fe + CNO collisions and almost five times as high as in the Fe + AgBr collisions.

A sufficiently simple possibility of detecting a residue nucleus is one of the advantages of studying the Fe + H events compared with the "mirror" events. As a result of studying the properties of the residue products of disintegrations at $Z = 23$-27, Rudstam [16]) proposed a formula to describe the yield of residue nuclei. The mean charge $\langle Z \rangle$ of residue nuclei may be expressed as $\langle Z \rangle = Z_p - 1/k$, where k is a fitting parameter which is 1.13 [ref. [9])] at $E_o = 2$ GeV. In our case the mean charge of residue nucleus in the Fe + H collisions was 17.7 ± 0.6, which is close to 18.3 the value given by the Rudstam formula. The strong dependence of parameter k on the mass of the interaction partner (the mean charge of residue nucleus in the Fe + CNO and Fe + AgBr collisions was 12.2 ± 0.5 and 9.8 ± 0.8 charge units, respectively) and the nonexponential distribution of fragment yields with increased fragment charges prevent the Rudstam formula from being used in the case of the Fe + CNO and Fe + AgBr interactions.

Using the fireball-model phenomenology [17]), we calculated the fragmentation parameters for interactions of iron nuclei with emulsion nuclei at 1.8 GeV/nucleon. In the fireball model, the fragment mass and charge are defined by the number of nucleons lost by a projectile nucleus during the fast interaction stage (N_{int}) and in the course of subsequent "cooling" (N_{ev}) of a produced excited residue nucleus. In this case we get

$$A_{fr} = A_p - (N_{int} + N_{ev}), \qquad Z_{fr} = Z_p - (Z_{int} + Z_{ev}),$$

where A_p, Z_p and A_{fr}, Z_{fr} are, respectively, the mass numbers and the charges of a projectile nucleus and of a produced fragment.

The number of knocked-out nucleons was inferred from the collision geometry on assumption that the nuclei are spheres with well-expressed boundaries and that all the projectile-nucleus nucleons appearing in the region of overlapping with the target nucleus suffer interactions and are emitted from the nucleus. The excitation energy of the residue nucleus was determined, according to ref. [18]), by the formula

$$E_{ex} = \alpha \Delta S, \tag{3}$$

where α is the surface-energy coefficient taken to be 0.95 MeV/fm^2; ΔS is the difference between the surface area of a produced residue-nucleus when a cylinder meets a sphere and the surface area of a sphere containing the same number of nucleons. We note that both the projectile Fe and the heavier target nuclei have matter distributions characterized by an exponential fall-off with increasing radius, not a hard-sphere edge as used here. This will make the spectrum of transferred energies softer than the one we have used in this work. We find that, typically, we require a harder transfer spectrum to match the data, however.

The evaporation of an excited nucleus was calculated using the scheme [9]) with the level-density parameter $a = \frac{1}{20}A$. The calculated fragmentation parameters are presented in parentheses in table 3. The statistical errors in the values do not exceed 3%. From table 3 it follows that the given model gives systematically overestimated values of the highly-charged fragment multiplicities and gives underestimated values of the yields of singly- and doubly-charged fragments. We are of the opinion that this circumstance has arisen from the low excitation energy ascribed to the residue nucleus, which is particularly evident from comparing between the experimental and calculated distributions of the number of fragments in an individual disintegration event (see fig. 1). The calculated mean energy of residue projectile-nucleus excitation in interactions with emulsion nuclei proved to be ~50 MeV, i.e., approximately 5 times as low as the energy necessary for the experimental α-particle and proton multiplicities to be accounted for. At the same time, it should be noted that the model reproduces correctly the trend in the variations of the residue projectile-nucleus charge with increasing the target mass. For example, the calculated $\langle Z \rangle$ values are 14.7 for Fe + CNO and 12.5 for Fe + AgBr interactions, whereas the experimental $\langle Z \rangle$ values for the events in the same targets are 12.2 ± 0.5 and 9.8 ± 0.8, respectively.

The angular distributions of the fragment particles can conveniently be characterized by mean emission angles $\langle \theta \rangle$ (see table 4). From the experimental data it follows that $\langle \theta \rangle$ decreases with increasing fragment mass and that there is a trend in the mean emission angle of composite particles to increase with target-nucleus mass. The increase is due mainly to a higher fraction of particles emitted at anomalously large angles. In the events with light nuclei, for example, $(8.4 \pm 0.2)\%$ of relativistic α-particles are emitted at angles exceeding 5°, while $(11.4 \pm 2.4)\%$ of such particles are observed in the Fe + AgBr interactions. In the latter case, 2% of all the doubly-charged particles are emitted at angles exceeding 10°. Obviously, the ejection of such fragments can hardly be explained by the stripping mechanism because this mechanism implies that the momentum transferred to a relativistic α-particle must exceed 1800 MeV/c.

TABLE 4

Mean emission angles (degrees) of fragments for 1.8 GeV/nucleon ^{56}Fe interacting with hydrogen, light and heavy nuclei, and with all nuclei of emulsion

Target	Type of fragment					
	p $(Z = 1)$	α $(Z = 2)$	L $(3 \leqslant Z \leqslant 5)$	M $(6 \leqslant Z \leqslant 9)$	H $(10 \leqslant Z \leqslant 19)$	vH $(20 \leqslant Z \leqslant 26)$
H	2.63 ± 0.07	1.94 ± 0.10	1.31 ± 0.17	1.37 ± 0.18	1.16 ± 0.12	1.03 ± 0.08
CNO	2.78 ± 0.04	2.50 ± 0.08	2.00 ± 0.15	1.44 ± 0.13	1.16 ± 0.08	1.10 ± 0.07
AgBr	2.52 ± 0.05	2.58 ± 0.12	2.24 ± 0.28	1.87 ± 0.39	1.01 ± 0.19	
em	2.63 ± 0.03	2.44 ± 0.07	2.00 ± 0.10	1.63 ± 0.11	1.08 ± 0.08	1.04 ± 0.08

A similar rise in the fraction of relativistic fragments emitted at large angles was observed as the impact parameter of interacting nuclei decreases. The fraction of the fragment α-particles whose emission angle exceeds 5° was $(12\pm2)\%$ and $(17\pm3)\%$ for the Fe+CNO and Fe+AgBr collisions, respectively, in the disintegrations corresponding approximately to the complete overlapping of one of the interacting nuclei (with $Q \leqslant 19$ for CNO and $Q \leqslant 15$ for AgBr target, where Q is the total charge of relativistic fragments) and was $(4\pm1)\%$ and $(6\pm1)\%$ for more peripheral nuclei $(Q > 19$ and $Q > 15)$.

The occurrence of particles of the above types in the system composed of the remaining projectile nuclei cannot be explained in terms of a simple "abrasion-ablasion" model [19] used to account for fragmentation of relativistic nuclei and necessitates other mechanisms of nucleus-nucleus interactions.

A new class of models currently under development is the multi-fragmentation model. This approach seeks to distinguish between sequential break-up of ever smaller systems and simultaneous break-up of a larger system into many small pieces. Randrup [20] has recently reviewed some of these approaches in an attempt to understand the time development of the fragmentation process. Such approaches may well help to explain the large number of events observed to have multiple complex fragments in the final state here.

5. Mean multiplicities of secondaries

Table 5 presents the mean multiplicities of the b-, g-, h- and s-particles produced in the collisions of ^{56}Fe nuclei with nuclei of different masses and compares the experimental and calculated (in parentheses) values for a singled-out class of

TABLE 5

Comparison of experimental mean multiplicities to those calculated using DCM (shown in parentheses) for different types of 1.8 GeV/nucleon ^{56}Fe interactions

Type of interaction	Fe + H	Fe + CNO	Fe + AgBr	Fe + AgBr $(n_h \geqslant 28)$	Fe + em
$\langle n_b \rangle$	0.12 ± 0.03	1.77 ± 0.10	6.63 ± 0.33 *	9.37 ± 0.56	4.07 ± 0.23
	(0.011 ± 0.003)	(1.57 ± 0.03)	(6.54 ± 0.11)	(9.14 ± 0.22)	(3.68 ± 0.08)
$\langle n_g \rangle$	0.26 ± 0.04	2.87 ± 0.14	13.66 ± 0.96	27.33 ± 1.34	8.23 ± 0.60
	(0.35 ± 0.01)	(3.93 ± 0.05)	(15.3 ± 0.3)	(31.8 ± 0.5)	(8.77 ± 0.24)
$\langle n_h \rangle$	0.38 ± 0.05	4.64 ± 0.13	20.29 ± 1.13	36.7 ± 1.30	12.30 ± 0.76
	(0.36 ± 0.01)	(5.49 ± 0.04)	(21.9 ± 0.5)	(40.9 ± 0.5)	(12.45 ± 0.38)
$\langle n_s \rangle$	2.50 ± 0.17	8.12 ± 0.50	14.01 ± 0.98	25.57 ± 1.33	10.53 ± 0.68
	(2.36 ± 0.05)	(9.53 ± 0.18)	(15.7 ± 0.4)	(31.8 ± 0.5)	(11.28 ± 0.32)
$\langle Q \rangle$	24.33 ± 0.15	20.05 ± 0.35	15.84 ± 0.69	8.06 ± 0.71	18.83 ± 0.43
	(24.74 ± 0.05)	(20.66 ± 0.13)	(18.05 ± 0.26)	(10.09 ± 0.28)	(19.03 ± 0.18)
$\langle n_s \rangle$	3.00 ± 0.19	3.9 ± 0.18	3.30 ± 0.20	4.35 ± 0.34	3.46 ± 0.18
	(4.85 ± 0.05)	(9.03 ± 0.07)	(4.88 ± 0.07)	(7.00 ± 0.10)	(6.44 ± 0.06)

interactions at small impact parameters ($n_h \geqslant 28$) and for the emulsion as a whole (Fe + em).

The increase of the multiplicity of various types of particles with rising target-nucleus mass can be explained by the power-law dependence $n \sim A^\alpha$, where $\alpha = 0.34 \pm 0.04$ for s-particles, 0.82 ± 0.06 for g-particles, and 0.68 ± 0.06 for b-particles. These values are very close to the values obtained experimentally with a ^{14}N beam of the same velocity [21]) (the respective values are 0.35 ± 0.03, 0.88 ± 0.05 and 0.77 ± 0.04). The agreement seems, however, to be accidental because the approximation was made in two works with respect to only three (in the case of s-particles) and two (in the case of g- and b-particles) experimental points. It may be claimed, nevertheless, that the character of the dependence of mean multiplicities of secondaries is almost independent (at least for $A_p = 14$–56) of the type of a projectile nucleus.

As the projectile mass increases, the g- and s-particle multiplicity increases too, while the number of low-energy particles (b-particles) remains in practice the same, or even decreases. For comparison, it should be indicated that the mean multiplicity of the b-, g-, and s-particles in the ^{14}N + AgBr interactions was found in ref. [21]) to be 7.25 ± 0.27, 8.51 ± 0.46, and 10.35 ± 0.40, respectively. In our case, the respective values for the ^{56}Fe + AgBr collisions proved to be 6.36 ± 0.33, 13.66 ± 0.96, and 14.01 ± 0.98, respectively. This means that the energy spectrum of protons from target nuclei gets harder with increasing projectile mass, which was indicated earlier ref. [22]). In this connection, it should be noted that a replacement of projectile nucleus (of ^{14}N by ^{56}Fe) gives rise to a substantial increase in the occurrence frequency of large ($n_h \geqslant 28$) disintegrations, namely, from $(16 \pm 2)\%$ to $(33 \pm 5)\%$.

Comparison between the experimental and the DCM-calculated mean multiplicities (see table 5) has shown that the given model can satisfactorily reproduce the mean yields of various types of particles. It should also be noted that the mean multiplicities in the calculated iron nucleus–hydrogen interactions are in better agreement with experimental data compared with the Fe + CNO and Fe + AgBr events. The calculated total charge of noninteracting fragments of a projectile nucleus (Q) is somewhat in excess of its experimental value. The difference arises mainly from the difference in the multiplicities of n_s stripping protons of projectile nucleus. Both experimental and calculated (not presented here) distributions of the numbers of definite types of particles are of a falling form typical of relativistic nucleus–nucleus interactions [23]) and prove to be in satisfactory agreement with each other. Some quantitative differences are observed in the multiplicity distributions of the "gray" and relativistic s-particles. For example, the fraction of disintegrations with $n_g \geqslant 5$ is $(23 \pm 4)\%$ in the calculated ensemble of the Fe + CNO interactions, whereas the experimental value is $(14 \pm 3)\%$. In the Fe + AgBr interactions, the calculated and experimental relative occurrence probabilities of events with $n_h \geqslant 28$ proved to be 0.38 ± 0.03 and 0.33 ± 0.05, respectively, while the fraction of events with $n_s \geqslant 40$ was $(11 \pm 2)\%$ and $(2.5 \pm 1)\%$. Similar overestimation of the relative contribution of

the interactions with strong disintegrations of colliding nuclei is also observed in the case of the "central" ($n_h \geqslant 28$) interactions for which the DCM-calculated values of $\langle n_s \rangle$, $\langle n_h \rangle$ and $\langle n_g \rangle$ are much in excess of their experimental values (see table 5).

6. Correlations of multiplicities

One of the effective methods for verifying the adequacy of a model describing nuclear interactions is to obtain the correlations among secondaries in a star. The g-particle multiplicity in a disintegration and the charge of noninteracting fragments of a projectile (Q), which characterize the degree of overlapping of two nuclei in a collision, were selected to be arguments (see figs. 2-5). The figures present the experimental data on the ^{56}Fe interactions with light and heavy nuclei of an emulsion,
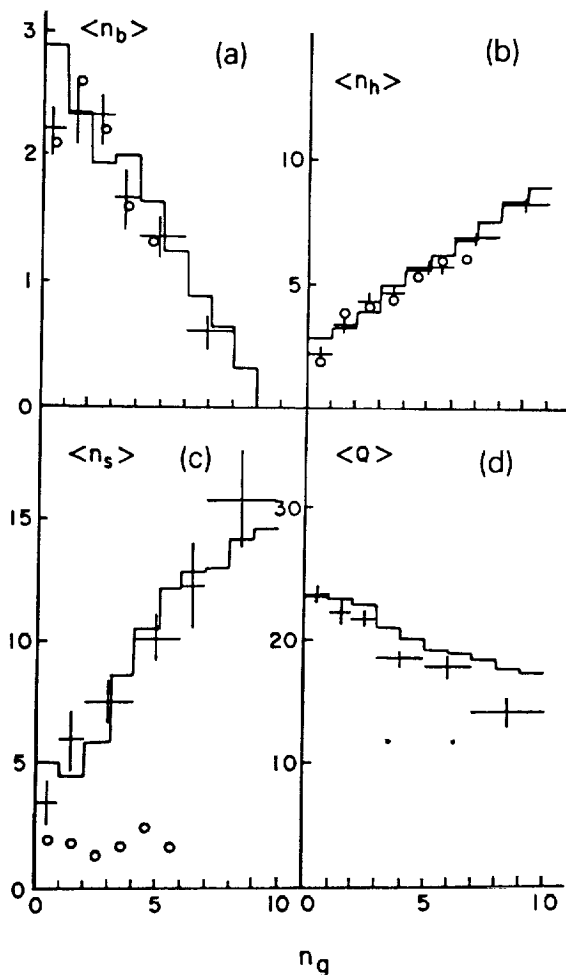
Fig. 2. Correlation functions versus n_g in nuclear interactions with CNO emulsion nuclei: (a) $\langle n_b \rangle$; (b) $\langle n_h \rangle$; (c) $\langle n_s \rangle$ and (d) $\langle Q \rangle$. The open dots are experimental data for projectile-proton at energy $E_0 = 3.6$ GeV/nucleon. The crosses are experimental data with error bars for ^{56}Fe at $E_0 = 1.8$ GeV/nucleon. The histograms are the DCM calculation results for ^{56}Fe at $E_0 = 1.7$ GeV/nucleon.
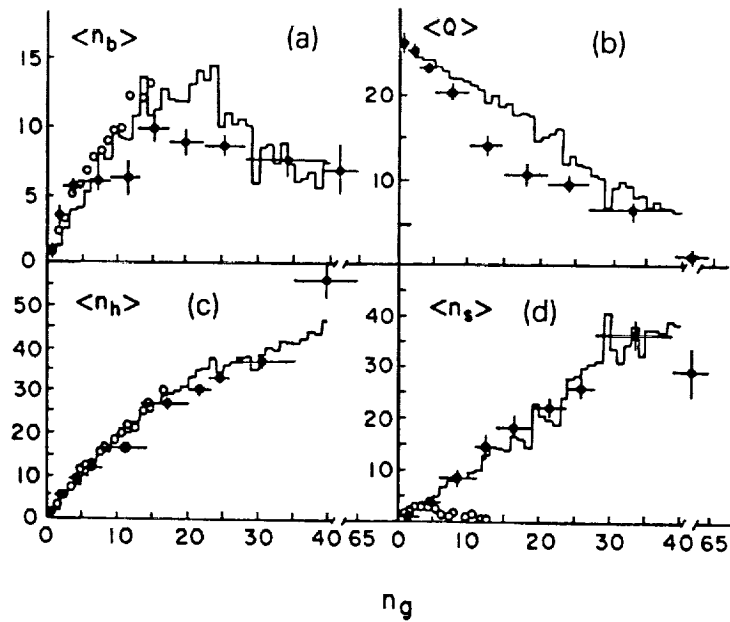
Fig. 3. Correlation functions versus n_g in nuclear interactions with AgBr emulsion nuclei: (a) $\langle n_b \rangle$; (b) $\langle Q \rangle$; (c) $\langle n_h \rangle$ and (d) $\langle n_s \rangle$. The open dots are experimental data for projectile-proton collisions at $E_0 = 3.6$ GeV [ref. [24]]. The full dots are experimental data for ^{56}Fe at $E_0 = 1.8$ GeV/nucleon. The histograms are the DCM calculation results for ^{56}Fe at $E_0 = 1.7$ GeV/nucleon.
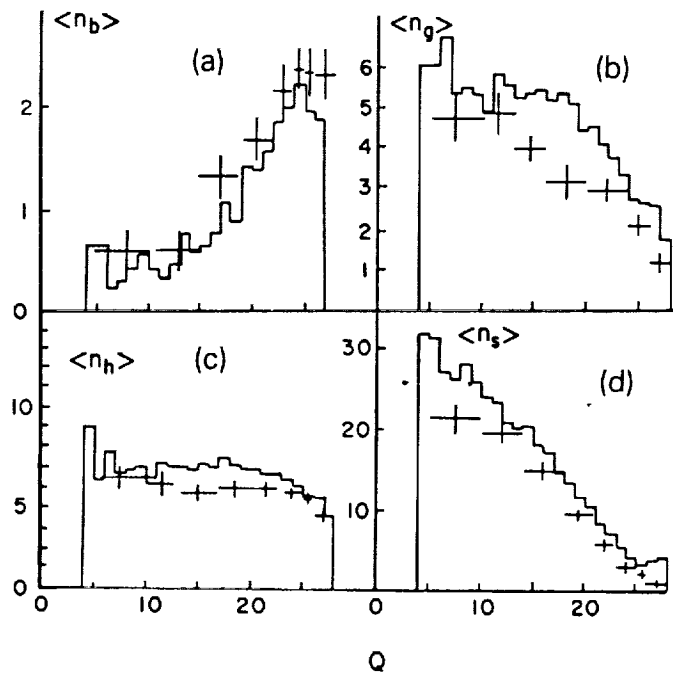
Fig. 4. Correlation functions versus Q in Fe + CNO interactions: (a) $\langle n_b \rangle$; (b) $\langle n_g \rangle$; (c) $\langle n_h \rangle$ and (d) $\langle n_s \rangle$. The dots are experimental data. The histograms are the DCM calculation results.
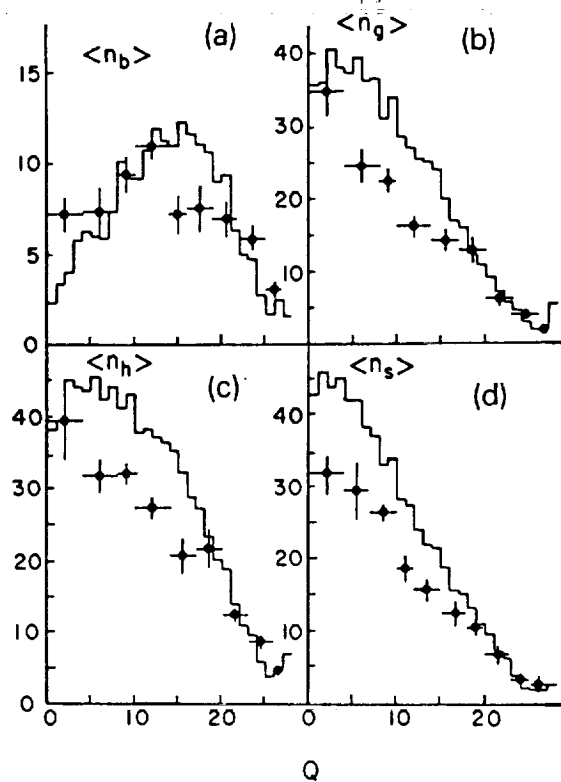
Fig. 5. Correlation functions versus Q in Fe + AgBr interactions: (a) $\langle n_b \rangle$; (b) $\langle n_g \rangle$; (c) $\langle n_h \rangle$ and (d) $\langle n_s \rangle$. The dots are experimental data. The histograms are the DCM calculation results.

the DCM calculation results, and the proton–nucleus interaction data [24]. The correlations of the $\langle n_g \rangle(Q)$ and $\langle Q \rangle(n_g)$ type make it possible to see the relationship between the arguments; namely, at small impact parameters the value of $\langle n_g \rangle$ (the number of target-nucleus protons knocked out during the fast interaction stage) is high, while the value of Q is at its minimum; as the impact parameter increases, the $\langle n_g \rangle$ value decreases, while the value of Q rises accordingly. The $\langle Q \rangle$ value can be used also to estimate the mean number of the projectile-nucleus protons involved in the fast reaction stage, namely, $n_{in} = 26 - \langle Q \rangle$. From the data of table 5 it may be obtained that the mean ratio of the numbers of protons involved in the fast reaction stage for the CNO, Fe and AgBr nuclei is $(0.48 \pm 0.06) : 1 : (1.34 \pm 0.16)$, i.e. 0.5 and 1.34 recoil protons are knocked out on the average from light and heavy target-nuclei, respectively, per single interacting nucleon of a projectile nucleus. The above ratio is close to the $Z_p^{2/3}$ dependence. Examination of the correlations $\langle Q \rangle(n_g)$ and $\langle n_g \rangle(Q)$ has shown, however, that in the case of peripheral nuclear collisions the ratio n_g/n_{in} of projectile is close to unity in the interactions with both light and heavy nuclei. In case of central collisions (small values of Q), the values of the n_g/n_{in} ratio are very different for different emulsion components and reach 0.22 ± 0.05 for the Fe + CNO collisions and 1.6 ± 0.2 for the Fe + AgBr collisions. The observed dependence of the ratios of interacting protons under nuclear collisions seems to us to

be associated with the rising importance of the secondary nucleon–nucleon interactions in the central nuclear collisions subject to finiteness of proton number in each of the colliding nuclei.

Having been normalized by a single interacting proton of a projectile nucleus, the multiplicity of relativistic s-particles appears to be 1.4 ± 0.1 and is the same for the target nuclei with very different masses (H, CNO, AgBr) and for a sampling of central events with $n_h \geqslant 28$. The correlation function $\langle n_s \rangle (Q)$ (figs. 4d and 5d) may also be presented as a straight line, $\langle n_s \rangle = 1.4 \times (26 - Q)$ in case of both light and heavy nuclei of an emulsion. This dependence of $\langle n_s \rangle$ on Q agrees with the model of independent interactions and is indicative of the decisive role of the first interaction of nucleons. The dependences $\langle n_s \rangle (n_g)$ for both components of emulsion are nearly linear with positive coefficients depending on target-nucleus mass and are absolutely at variance with the proton–nucleus interaction data; that is, the mean multiplicity of s-particles in the p + CNO interactions is in practice independent of the number of "gray" particles (figs. 2c and 3d), while the correlation function $\langle n_s \rangle (n_g)$ in the p + AgBr interactions exhibits even a trend to decrease.

Visual correlation between the fast and slow stages of the reaction of inelastic interaction of two nuclei may be obtained by examining a correlation of the $\langle n_b \rangle (n_g)$ form (figs. 1a and 3a). The form of this dependence in the case of heavy nuclei shows that it is approximately linear at a small g-particle number which can be related to the low degree of cascading in target nucleus, i.e., the emission of each g-particle makes, on the average, the same contribution to the excitation energy.

The same correlation in the p + AgBr interactions exhibits a stronger dependence (figs. 1a and 3a), thereby indicating that the g-particles in nucleon–nucleus collisions excite the target-nucleus more effectively. The small n_g values in nucleus–nucleus interactions correspond to high impact parameters when the colliding nuclei touch each other but slightly, so the g-particles are protons knocked out from the extreme periphery of a heavy nucleus. The same number of "gray" rays in the proton-produced star correspond to low impact parameters, to more intensive cascading, and, hence, to higher excitations of target-nucleus. At high n_g values (above 15), i.e. in the region attainable only in nucleus–nucleus interactions, the mean multiplicity $\langle n_b \rangle$ not only is independent of the number of "gray" rays in a star, but also exhibits a trend to decrease. Two factors are notable among the reasons for the above described $\langle n_b \rangle (n_g)$ behaviour. The first factor is the above-mentioned "finiteness" of a target-nucleus. If a target-nucleus loses 20–25 protons during the fast reaction stage (the inflexion zone of the correlation function $\langle n_b \rangle (n_g)$, see fig. 3a), a "lack" of nucleons is observed in the target-nucleus residue during the second, "slow", stage. The second factor consists of the high excitation energies of the residue nuclei of targets which may give rise to an explosion-like process of secondary particle emission, thereby resulting in their acquiring an energy exceeding the energy boundary of the "black" rays. The effect of the two factors appears to be most visual in the case of the correlation function $\langle n_b \rangle (n_g)$ under interactions of iron nuclei with light nuclei of an emulsion. Here, an increase of the number of "gray" rays in a

star leads in practice to the complete disappearance of b-particles in a disintegration (fig. 2a). The character of the dependences $\langle n_b \rangle (Q)$ (figs. 4a and 5a) is the same as the behaviour of the correlation function $\langle n_b \rangle (n_g)$ (figs. 2a and 3a), so they are most probably defined by identical factors.

From figs. 2–5 it is seen that the DCM can rather well reproduce the behaviour of the experimental correlations. Some differences are observed in the Q-dependences (figs. 4 and 5). The following trend can be noted in this case: the DCM reproduces quite properly the experimental data at high values of the total charge of the projectile-nucleus fragments ($Q > 18$), which correspond to peripheral interactions. In the case of central interactions, the DCM overestimates the mean multiplicities of secondaries. On the other hand, the form of the $\langle Q \rangle (n_g)$-type inverse correlations shows that the model predicts higher values of $\langle Q \rangle$ under a significant destruction of target-nucleus compared with experimental data. It should also be noted that the differences between experimental and calculated values manifest themselves more pronouncedly in the Fe + AgBr interactions compared with the Fe + CNO reactions.

Since the Q-values summarize the stripping fragments of a projectile nucleus with $Z = 1$, which differ only in angle, they may include the produced particles whose model-predicted mean multiplicity is fairly high (see table 5). Obviously, if this excessive meson production could have been suppressed in the model, the agreement between the experimental and calculated mean s-particle multiplicities would have been much improved and, in addition, a better agreement between the $\langle n_s \rangle (n_g)$ and $\langle Q \rangle (n_g)$ correlation functions would have been attained. The inclusion of the πN and NN resonances [25] in the calculations may substantially diminish the cascade branching and, accordingly, the secondary-particle multiplicity would decrease. The inclusion of the above resonances is particularly important in the case of collisions of heavy nuclei. The disagreement between the experimental and calculated dependences $\langle n_i \rangle (Q)$ may also arise from using the statistical evaporation theory, which seems to be ineffective at small impact parameters of nuclei, to describe the characteristics of particles emitted from the projectile nucleus. It should also be noted that the given version of the model disregards the distortions of projectile trajectories by Coulomb forces and neglects the momentum transfers to interacting nuclei, as a whole, in a collision; i.e., the model fails to allow for the effects which become noticeable under collisions of heavy nuclei. The allowance for the above-mentioned factors may result in a decreased probability of interactions at small impact parameters; i.e., in a lower occurrence frequency of many-ray stars; besides, it will decrease the Q-value and improve, in this way, the degree of agreement between the calculated and experimental data.

7. Conclusions

The following conclusions may be drawn from the results of the present work and from the subsequent analysis.

(i) The experimental cross sections for inelastic interactions of 1.8 GeV/nucleon iron nuclei with photographic emulsion nuclei may be described in terms of the Bradt–Peters geometric model and prove to agree satisfactorily with the DCM-calculated cross sections.

(ii) The fragmentation parameters of iron nuclei depend strongly on partner-nucleus mass. In this case the fraction of disintegrations with multicharged fragments ($Z \geqslant 3$) decreases with increasing the target-nucleus mass. Emission of two or more $Z \geqslant 4$ fragments was observed in $(12 \pm 3)\%$ of the Fe + H interactions.

(iii) The charge distribution of residue nuclei in the Fe + H collisions may be described by the Rudstam formula which, however, appears to be inapplicable to the Fe + CNO and Fe + AgBr interactions.

(iv) Theoretical calculations obtained in terms of the model described by Gosset et al.[18]) disagree with experimental data. The excitation energy ascribed by the calculations to the residual nucleus leads to disagreement with the experimental multiplicity of "evaporation" particles.

(v) The angular distributions of projectile fragments comprise particles with anomalously large emission angles. The fraction of such particles increases with target-nucleus mass.

(vi) The dependences of the mean b-particle multiplicity, or Q, are of different forms for target-nuclei of different masses. The effect of the "finiteness" of a heavy target nucleus, which is not observed in nucleon-nucleus interactions, manifests itself in the Fe + AgBr interactions.

(vii) The analysis of the correlation functions of particle multiplicities in a disintegration has shown that the simple superposition model for nucleon–nucleus interactions is inapplicable to the nucleus–nucleus interactions. The model assumes a linear dependence between the number of secondaries and the number of interacting projectile nucleons. This type of dependence is observed only in the case of s-particles, but does not take place in the case of b- and g-particles.

(viii) The DCM describes qualitatively all the experimental data examined. A quantitative agreement is observed with the results for Fe + H reactions and in the case of peripheral Fe + CNO and Fe + AgBr interactions. To get a better description of central collisions at small impact parameters, the model must be further refined.

References

1) R. Stock, Nucl. Phys. A434 (1985) 537
2) W. Gelbrath and W.C. Williams, High energy and nuclei physics data handbook (Chilton, 1963)

106

3) V.A. Antonchik, V.A. Bakaev, S.D. Bogdanov, A.I. Vikhrov, V.E. Dudkin, V.V. Iroshnikov and N.A. Nefedov, Yad. Fiz. (Sov. J. Nucl. Phys.) **35** (1982) 1103

4) B.P. Bannik et al., J. of Phys. **G14** (1988) 949

5) V.A. Antonchik et al., Yad. Fiz. (Sov. J. Nucl. Phys.) **28** (1978) 435

6) K.K. Gudima and V.D. Toneev, Yad. Fiz. (Sov. J. Nucl. Phys.) **27** (1978) 658

7) K.K. Gudima, H. Iwe and V.D. Toneev, J. of Phys. **G2** (1979) 237

8) K.K. Gudima and V.D. Toneev, Nucl. Phys. **A400** (1983) 173c

9) V.S. Barashenkov and V.D. Toneev, Interaction of high-energy particles and atomic nuclei with nuclei (Atomizdat, Moscow, 1972)

10) H.L. Bradt and B. Peters, Phys. Rev. **77** (1950) 54

11) G.D. Westfall, L.W. Wilson, P.J. Lindstrom, H.J. Crawford, D.E. Greiner and H.H. Heckman, Phys. Rev. **C19** (1979) 1309

12) A.H. Viniczkiy et al., Joint Institute of Nuclear Research Preprint, Dubna, P1-80-473, 1980

13) P.J. Lindstrom, D.E. Greiner, H.H. Heckman, B. Cork and F.S. Bieser, Lawrence Berkeley Laboratory Report No LBL-3650 (1975)

14) O.V. Logkin and N.A. Perfilov, Nuclear chemistry (Nauka, Moscow, 1965)

15) O.V. Logkin, Zh. Exsp. Teor. Fiz. (Sov. J. Exp. Theor. Phys.) **33** (1957) 354

16) G.Z. Rudstam, Z. Naturforsch. **27a** (1966) 1027

17) G.D. Westfall, J. Gosset, P.J. Johansen, A.M. Poskanzer, W.G. Meyer, H.H. Gutbrod, A. Sandoval and R. Stock, Phys. Rev. Lett. **37** (1976) 1202

18) J. Gosset, H.H. Gutbrod, W.G. Meyer, A.M. Poskanzer, A. Sandoval, R. Stock and G.D. Westfall, Phys. Rev. **C16** (1977) 629

19) M. Bleszynski and C. Sander, Nucl. Phys. **A326** (1979) 525

20) J. Randrup, Nucl. Phys. **A495** (1989) 245c

21) G.M. Chernov et al., Nucl. Phys. **A280** (1977) 478. [Also: G.M. Chernov et al., Dokl. Izbec. Akad. Nauk. **2** (1977) 20 (in Russian)]

22) V.A. Antonchik, V.A. Bakaev, S.D. Bogdanov, A.I. Vikhrov, V.E. Dudkin, N.A. Nefedov, V.I. Ostroumov and Yu.V. Potapov, Yad. Fiz. (Sov. J. Nucl. Phys.) **33** (1981) 1057

23) V.A. Antonchik et al., Yad. Fiz. (Sov. J. Nucl. Phys.) **33** (1981) 3; 1057

24) M.I. Adamovich et al., High Energy Physics Institute of Kazach Academy of Sciences Preprint, Alma-Ata, No 81-11, 1981

25) V.S. Barashenkov et al., Joint Institute of Nuclear Research Preprint, Dubna, P2-83-117 (1983)